Cryogenics 143 (2024) 103951

Contents lists available at ScienceDirect

Cryogenics

journal homepage: www.elsevier.com/locate/cryogenics

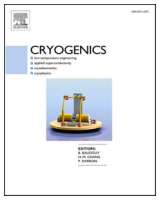

Cryogenic thermosiphon used for indirect cooling of superconducting magnets

Weronika Głuchowska [a,b], Tomasz Banaszkiewicz [b,*], Matthias Mentink [a], Benoit Cure [a], Alexey Dudarev [a], Shuvay Singh [a]

[a] CERN, European Organisation for Nuclear Research, 1211 Geneva 23, Switzerland
[b] Wroclaw University of Science and Technology, Wybrzeze Wyspianskiego 27, 50 - 370 Wroclaw, Poland

ARTICLE INFO

Keywords:
Helium
Superconductive magnets
Thermosiphon
Cryogenics

ABSTRACT

A thermosiphon is a thermodynamic phenomenon that facilitates the circulation of cryogen within a cooling system, relying solely on gravitational forces and phase change. This mechanism leverages the variations in the density of the cryogenic fluid throughout the entire cooling loop, creating a pressure gradient. This gradient serves as the primary driving force for the circulation of the cryogen. To negate the necessity of a circulation pump, it is crucial to determine the geometry of the cooling loop, the configuration of the thermosiphon, its height, and the vertical placement of the cryogen phase separator. This paper introduces a simplified computational model and the geometric calculations of the cryogenic thermosiphon for two distinct configurations of the indirect cooling loop for superconducting magnets.

1. Introduction

Historically, high magnetic field superconducting magnets have extensively relied on low- temperature superconductors (LTS), in particular Niobium-Titanium alloy, which features a critical temperature of 9.2 K and a critical magnetic field of about 15 T [1–3]. For magnetic field applications of up to a few Tesla, this alloy is thus compatible with the boiling temperature of liquid helium, equal to 4.2 K at atmospheric pressure [4]. One of the most crucial aspects of the LTS coil construction is designing an efficient cryogenic cooling circuit. Various factors must be considered in the cryogenic design, including reliability and low electrical power consumption. By addressing these factors, the aim is to achieve cost-efficiency, reliability, redundancy, and, ideally, limited complexity. The thermosiphon-based cooling method is found highly reliable since being created as a passive cooling method, it does not require the usage of mechanical pumps to generate mass flow in cooling pipelines. For this reason, it has been successfully applied to several cooling systems of high-field superconducting detector magnets, such as the ALEPH Solenoid [5,6], the ATLAS Compact Solenoid [7], and the Compact Muon Solenoid (CMS) operating at CERN [8]. Due to its demonstrated feasibility and reliability, thermosiphon remains an attractive method for cooling superconducting facilities that are currently under study. Examples of those include, among others, the Production Solenoid at Fermilab [8,9], the ARIEL cryomodules for 1.3 GHz superconducting cavities at TRIUMF [10], and the PANDA Solenoid at FAIR [11]. In principle, such cooling loops can be designed in Zero-Boil-Off configuration (ZBO), where cryocoolers locally condensate a cryogen which is subsequently circulated using the thermosiphon phenomenon [12,40]. One major benefit of this solution is that ZBO cryostats can operate without being permanently connected to a cryogenic distribution system which decreases the complexity of the facility, investment cost, and helium consumption while increasing its reliability [13–15]. Therefore, it is believed that further development of the thermosiphon-based cooling systems combined with the ZBO concept is highly promising for the future of high-field superconducting facilities.

The core aspect of the design of the thermosiphon-based cooling system, which is also the main topic of this paper, is to determine its hydraulic characteristics during nominal operation, which depends on the geometry of the cooling tubes and their spatial orientation. Two main tubing configurations can be found in the literature: horizontal and vertical, with the second option used more frequently.

An example of the horizontal configuration is the cooling system of the ATLAS Compact Solenoid, where the inner cooling circuit consists of two parallel-connected serpentines attached to the outer surface of the magnet's cold mass [7,41] (see Section 3.1).

The horizontal configuration was implemented in the Compact Muon

* Corresponding author.
E-mail address: tomasz.banaszkiewicz@pwr.edu.pl (T. Banaszkiewicz).

https://doi.org/10.1016/j.cryogenics.2024.103951
Received 12 February 2024; Received in revised form 21 June 2024; Accepted 17 September 2024
Available online 19 September 2024

Solenoid. In this case, the inner cooling circuit consists of 8 independent modules, each including 12 vertically oriented tubes attached to the cold mass and connected by the top and the bottom manifold [8,16,41] (See section 3.2).

Both geometrical configurations have been the subject of research in the context of heat transfer and hydraulics in the cooling systems of LTS magnets. Several mathematical models were formulated and tested to describe two-phase flow in helium for both vertical and horizontal orientations. The conducted experiments demonstrate the validity of certain models, like the separated flow or the homogenous model and constitute a source for considerations on the thermosiphon phenomenon [17–22]. Several works introduce an analytical approach to the design of thermosiphon-based cooling systems in the vertical configuration. These works present both mass and heat transfer for single cooling loops [9,22,23] as well as selected problems in the design of more complex cooling loops for superconducting magnets [6]. In contrast, similar considerations regarding horizontal tubing and, above all, detailed differences between the two configurations have not been found.

Therefore, it was chosen to consolidate the collected information on this topic and formulate a simplified mathematical model that can be used to perform hydraulic calculations of the thermosiphon-based cooling systems for LTS magnets for both vertical and horizontal configurations. The additional motivation of this paper is to indicate the differences between those two for the same thermal loads of the cold mass. The formulated mathematical model will be experimentally validated in the test campaign in 2025, where thermosiphon-based cooling will be integrated into the ZBO configuration. In this paper, Section 2 shows the different methods used currently for cryostating superconductive magnets. Section 3, describes two analyzed geometries of the cooling circuit of a superconducting magnet. Section 4 presents a mathematical model that allows determining the parameters of a cryogenic thermosiphon depending on its geometry. Section 5 illustrates the results of the model calculations for various computational parameters. The analysis is summarized in Section 6.

2. Superconducting magnet cooling

The main heat inputs to the LTS superconducting magnet, operating below 5 K, result from heat radiation from surrounding objects held at higher temperatures (i.e. thermal shields), heat conduction through the support structure, and magnet current leads (if they are not sufficiently thermalized) [4]. This energy must be captured by the continuously running cooling system to sustain the magnet under its nominal operating conditions. Currently one can distinguish three primary liquid helium-based methods that are commonly employed for the operation of superconducting magnets: bath cooling, forced flow cooling and thermosiphon cooling [24].

2.1. Bath cooling

In this method of cooling, a superconducting coil is entirely submerged in a liquified cryogen, as shown in Fig. 1. The magnet is cooled down by the heat exchange with a stationary fluid. This concept is being successfully employed for small laboratory setups, MRI magnets, and big superconducting facilities such as detectors or accelerator magnets [4,25,26]. One of the advantages of this solution is the simplicity of its design. On the other hand, drawbacks include the large volume of cryogen that is rapidly evaporated during quench and the need for a large-volume vessel surrounding the cold mass. This method is also referred to as direct cooling.

2.2. Forced flow cooling

In the forced flow cooling method the cryogen stream is forced to flow through the heat exchanger thermally connected to the cooled mass. This concept can be based either on two-phase flow or one-phase

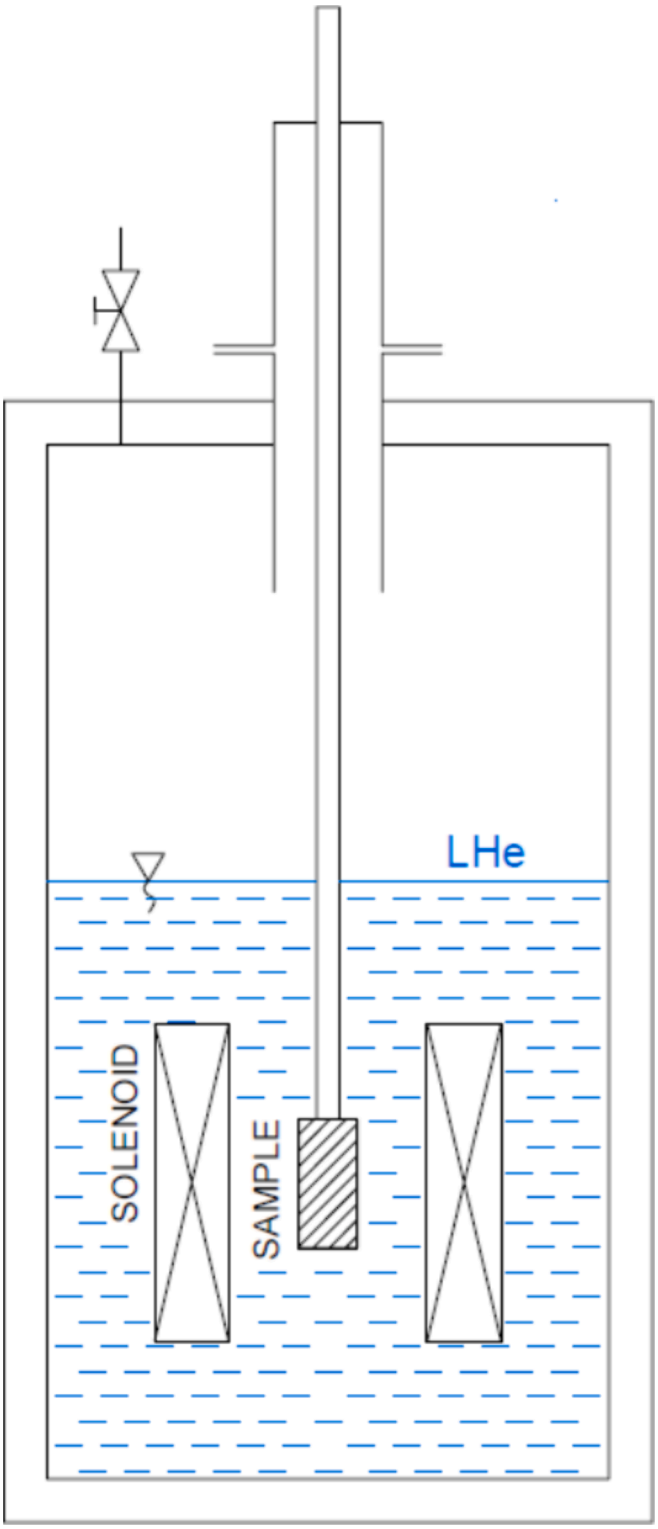

Fig. 1. Simplified scheme of the bath cooling system.

flow, either He-II or He-I can be used for this method [27]. The forced flow is obtained by mechanical pumps or by utilizing the thermomechanical effect of the He-II. The cryogen circulates in a closed cooling loop, as shown in Fig. 2. It requires the employment of a separated heat exchanger that stays in thermal contact with the cold mass. Since this method relies on the thermal contact between the cold mass and the cooling tubes, it is considered indirect cooling. In some special cases, superconducting cables are designed to enable helium flow inside them,

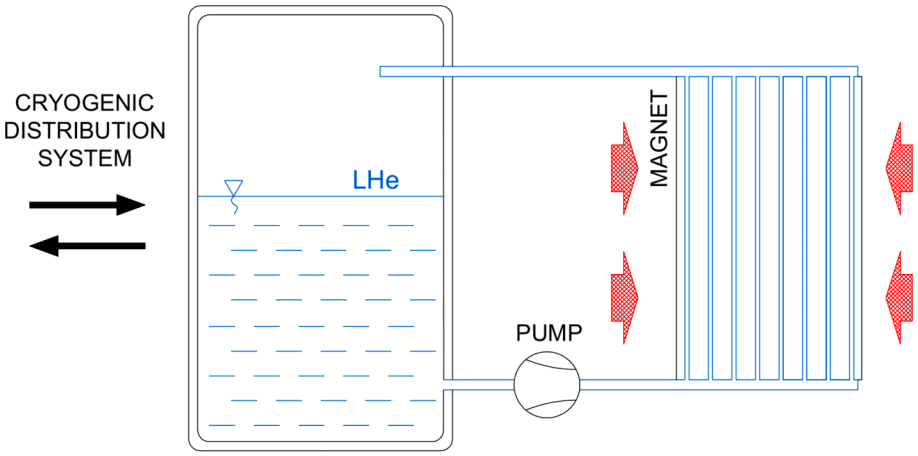

Fig. 2. Simplified scheme of the forced cooling system.

thereby creating direct thermal contact between the cold mass and the cryogen [28,29]. The advantage of this solution is that a smaller volume of cryogen evaporates in the case of a quench and that the need for a large-volume vessel surrounding the cold mass is avoided. The employment of mechanical pumps could be a disadvantage since the stoppage of the pump without a suitable backup system would result in a stoppage of cooling, and the pump gives a significant heat load to the liquid helium [30].

2.3. Thermosiphon cooling

This method is also based on the indirect cooling principle since there is no contact between the cryogen and the cold mass. In this case, mechanical pumps are replaced by the basic physical phenomenon which is referred to as the thermosiphon [12,39,40,42,43]. Under steady-state conditions, the heat leak to the magnet (indicated by the red arrows in Fig. 3) is transferred to helium (He-I) causing some portion of the helium stream to evaporate. The difference in vapour fraction, and thus the densities, between the supply and the return pipes drives the helium flow. Compared with the methods presented above, this method seems to be particularly attractive. For example, for nominal operation at 4.2 K, neither circulating pumps nor any external actions are required. As a result, maintenance frequency decreases, cost efficiency increases due to lower power consumption, and cryogenic reliability is increased because the cooling is not immediately affected by a power cut or pump failure. The drawback of that method is that it needs large vertical space. The liquid cryogen in the phase separator needs to have enough gravitational potential energy to force the stream through the entire cooling loop. Additionally the design and the geometry of the entire cooling loop, including pipe length, diameters and especially the height of the phase separator placement above the ground level need to be carefully and thoughtfully calculated. This is even more important than in the forced flow method as there is no possibility to incorporate the larger pump if the higher cryogen stream is needed.

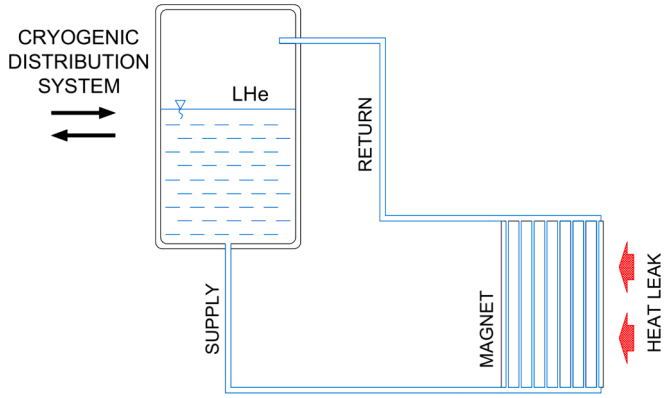

Fig. 3. The simplified scheme of the thermosiphon-based cooling system.

3. Thermosiphon

The operation principle of thermosiphon draws on basic fluid mechanics. The driving force of the thermosiphon is the difference in density between the supply and the return of the cooling system. This phenomenon is illustrated in Fig. 4.

The downward branch represents the supply, and the upward branch represents the return. They are both connected to the phase separator

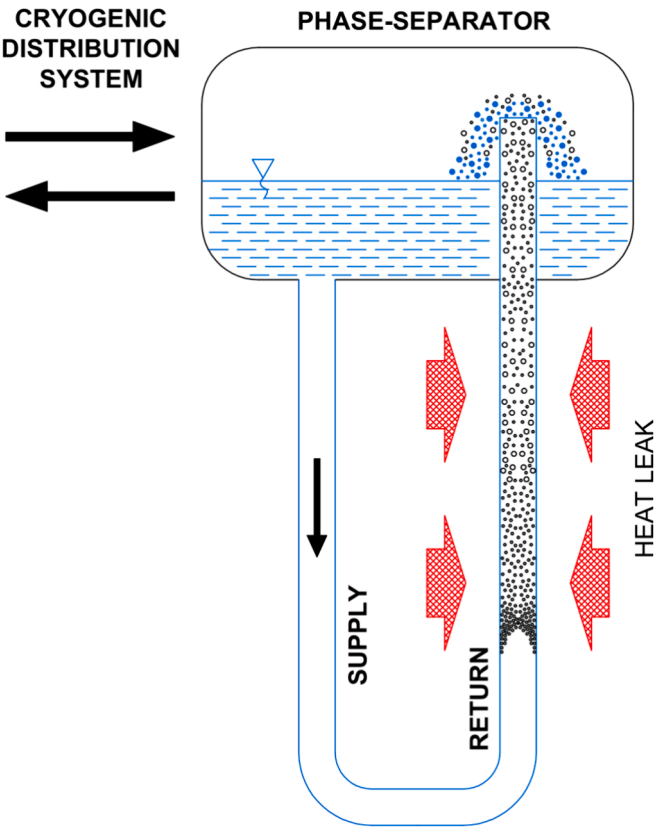

Fig. 4. The basic thermosiphon cooling loop.

located above the cooled object to provide a pressure head that initiates cryogen circulation. The heat inleak from the magnet to helium in the heat exchanger (represented in Fig. 4 by red arrows) causes helium to evaporate. Helium vapour fraction increases, and thus the helium density decreases. Since the mixture experiences lower gravitational force than the pure liquid flowing through the downward branch, helium starts circulating in the loop under the heat load. A properly designed system does not require the use of mechanical pumps for sustaining the flow of the coolant, although the flow itself needs to be initially triggered by the head pressure. For this reason, it is crucial to determine the minimum height of the phase separator placement which provides the mass flow in the system as well as compensates for the pressure drop through the pipelines created by friction. An important feature of thermosiphon cooling is even temperature distribution in the helium pipe since the evaporation process is quasi-isothermal [16,22,31] – the pressure difference in the cooling pipe throughout the cooling loop is minuscule.

The heat exchanger, indicated in Fig. 4 by the red arrow symbols in reality can have different geometry depending on the design of the cooled mass. As mentioned earlier the two most popular cooling loop geometries are the vertical and the horizontal cooling loop geometries. To formulate and implement a consistent mathematical model, the two thermosiphon-based cooling circuits were studied. Both heat exchangers are designed to maintain an operating temperature of about 4.5 K. For this purpose, a generic magnet was selected, featuring a cold mass with an outer area of 500 m^2, and a radiative heat flux onto the cold mass of 0.2 W/m^2 considered. The magnet geometry was selected based on the existing magnets operating at CERN, in particular, the CMS [7,32]. It is the superconductive solenoid made from an Al-stabilised conductor and it is confined within the Al support structure. These design concepts give good transparency for the particles passing through, as well as a light-cold-mass weight and a simple coil structure. The paper considers an aluminium-stabilised conductor because it is a typical candidate for indirect cooling. The coil is impregnated with epoxy and surrounded by an aluminium support cylinder to which cooling pipes are welded. The support cylinder also distributes temperature uniformly along the coil. Such a solution was chosen as it was already implemented, tested, commissioned, and is still operating not only in the case of the CMS detector but also, for example, the ATLAS solenoid [41].

3.1. Serpentine model geometry

The first geometrical configuration is the horizontal model referred to in the paper as the serpentine model. The exemplary view of the geometry is presented in Fig. 5 and Fig. 6. As shown, the cooling tubes with the serpentine configuration are attached to the outer surface of the support cylinder. The cooling path is divided into two parallel branches that meanders back and forth throughout the entire length of the cold mass. Helium flows between two distributive and mixing tees placed respectively at the bottom and the top of the support cylinder. Each horizontal section is slightly inclined to avoid vapour accumulation along the cooling path.

The main geometrical characteristics of the inner cooling circuit of the serpentine model taken into consideration during the analysis are listed in Table 1.

3.2. Vertical model geometry

The second geometry considered in this paper is the vertical model. The overview of the vertical geometry is shown in Figs. 7 and 8. The vertically oriented cooling tubes are attached to the outer-facing surface of the support cylinder. Each of the cooling tubes of the vertical model is bent in the shape of a semicircle and flows directly from the bottom to the top of the cylinder. To cover the entire area of the cooled cylinder, many of the small cooling tubes are used.

The cooling tubes are organized in groups and connected to their manifolds on the top and the bottom. The grouping of the cooling tubes is to minimize the diameters of the manifolds. In the analysed geometry the cooling circuit consists of 4 independent subcircuits, each including 10 vertical tubes connected to the top and bottom manifolds. The main geometrical characteristics of the inner cooling circuit of the vertical model taken into consideration during the analysis are listed in Table 2.

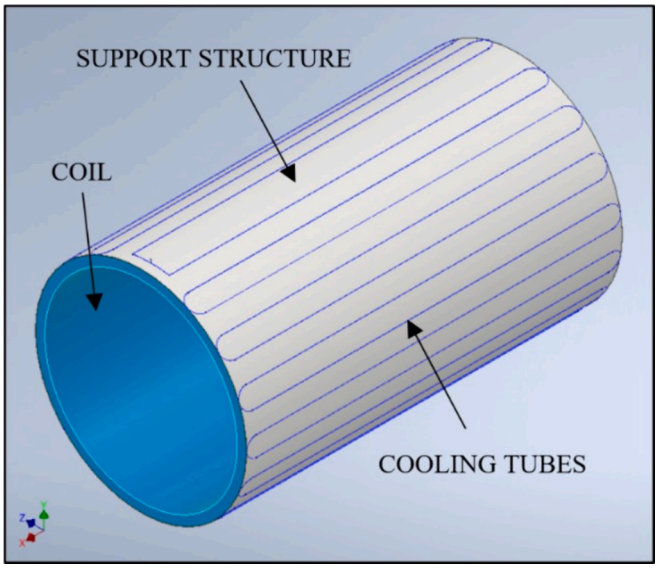

Fig. 5. 3D model of the serpentine cooling circuit (illustrative drawing).

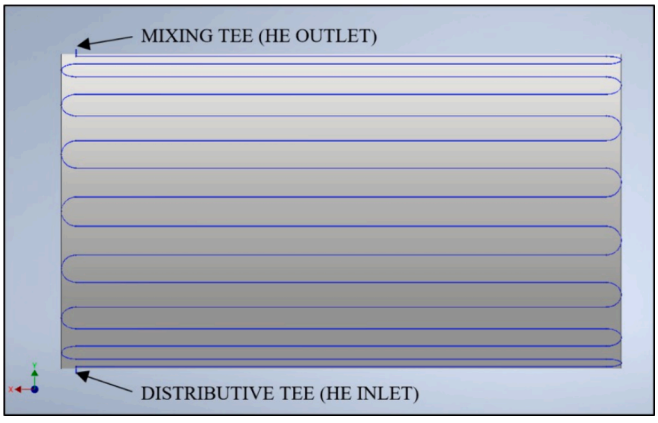

Fig. 6. Side view of the serpentine cooling circuit(illustrative drawing).

Table 1
Geometric characteristics of the serpentine cooling circuit.

Configuration: Serpentine	Value	Unit
Number of independent modules	1	–
Number of parallel branches	2	–
Number of horizontal sections	16	–
Spacing between horizontal sections	610	mm
Pipe length of a single branch	205	m
Inner diameter of the cooling tubes	16	mm
Outer diameter of the cooling tubes	18	mm

4. Mathematical model

4.1. Basic assumptions

There are two possible ways of describing the thermosiphon mathematically: separated model and homogeneous model. As the name

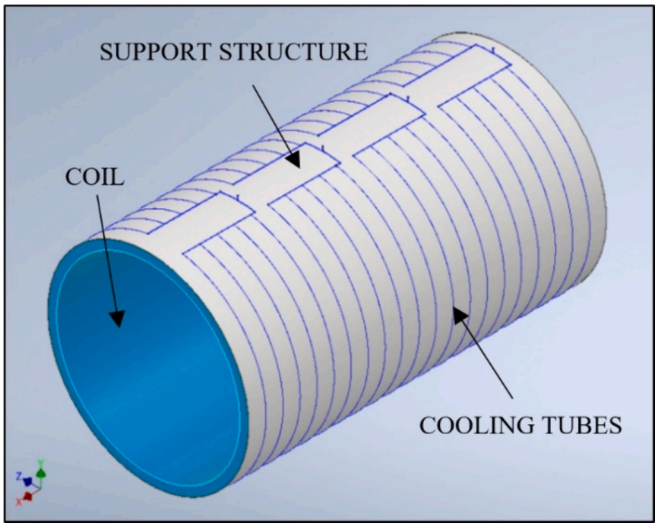

Fig. 7. 3D model of the vertical cooling circuit (illustrative drawing).

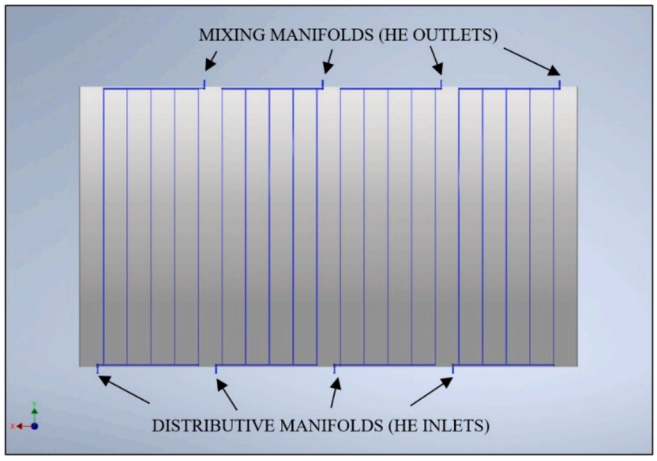

Fig. 8. Side view of the vertical cooling circuit (illustrative drawing).

Table 2
Geometric characteristics of the vertical cooling circuit.

Configuration: Vertical	Value	Unit
Number of subcirquits	4	–
Number of vertical tubes per single subcircuit	10	–
Pipe length of a single vertical branch	15	m
Inner diameter of the cooling tubes	16	mm
Outer diameter of the cooling tubes	18	mm
Inner diameter of the manifolds	36	mm
Outer diameter of the manifolds	40	mm
Spacing between cooling tubes	590	mm

suggests, the separated model imposes an individual consideration of the flow phases. It means that the vapour and the liquid flow at different velocities. The characteristic variable of this model is the ratio of the vapour velocity to the liquid velocity, known as the slip ratio. Its value is always greater than one since the vapour flows faster than the liquid. The homogeneous model, on the other hand, considers the two-phase mixture as a single fluid assuming mean fluid properties for further calculations. Such simplification can be undertaken based on three basic assumptions [33,34]:

- the liquid phase and the gas phase have the same velocities (the slip ratio of 1)
- the considered system is in a state of thermodynamic equilibrium
- the friction factors may be reasonably approximated through equations dedicated to single-phase flow

It is proven by several experimental works that the homogeneous model provides a good agreement for frictional pressure drop calculations with measurements for horizontal and vertical flow paths up to 60 % vapour fraction [16,17,20,31,39–43]. Generally, this model is found accurate for the nucleate boiling regime, i.e. until the film boiling appears, where the assumption of thermodynamic equilibrium between two phases does not stand anymore [31]. For this reason, the homogeneous model is considered a reasonable approximation which is applied in the mathematical model and further calculations of pressure drop. Furthermore, it was crucial to make another basic assumption which allows for determining thermodynamic parameters such as temperature, vapour fraction and pressure with sufficient precision. For this purpose, one assumes a single cooling branch to be a linear element of a particular length l that can be divided into a finite number of elements of the same lengths l_n as presented in Fig. 9.

The heat load $\dot{Q}$ is assumed to be distributed uniformly along the branch. The unit heat per element $\dot{Q}_n$ corresponds to the length l_n. Based on the above-mentioned assumptions, thermodynamic parameters such as temperature, vapour fraction and pressure can be calculated for each node x_n. Thus, knowing the inlet pressure and the pressure drop through each l_n-long section one can easily calculate the pressure drop through the whole branch. Once the pressure drop is defined, the minimum height can be determined based on the principle of communicating vessels. This principle refers to a fluid contained in a single vessel or connected vessels in a gravity field where horizontal planes create surfaces of constant pressure [35].

4.2. Input data

Derived from the presented assumptions, the simplified engineering mathematical model was formulated and implemented utilizing the Python programming language [36]. The properties of the working fluid were acquired through the Cool Prop database [37]. Various input variables are detailed in Table 3. In addition to those presented in the table, the detailed geometry of the cooling loop was incorporated into the calculations. This geometry is introduced in the form of a list of components with corresponding geometric features, such as the inner diameter of cooling tubes, the initial inclination of the tube, and other relevant characteristics.

4.3. The outlet vapour fraction for a single node of the calculation

The unit heat per element $\dot{Q}_n$, has two effects on helium. First is heating the helium to the boiling temperature at the given pressure which can be expressed using Equation (1).

$$\dot{Q}_n = \dot{m}_b C_p \Delta T \tag{1}$$

where:

$\dot{Q}_n$ – unit heat per element [W].

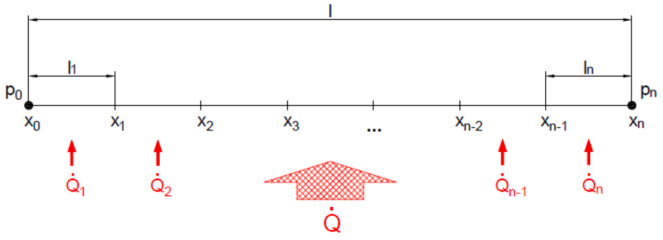

Fig. 9. The simplified scheme of a single branch divided into n number of elements.

Table 3
Input variables to the calculation software.

Variable	Unit	Definition
T	K	The operating temperature of the cryogen
x_n	–	Vapour fraction at the inlet of the cooling path
$\dot{Q}$	W	The total heat load
$\dot{m}$	g/s	Outflow from the phase separator
f	m	Mesh size (the length of a single element)
s	–	Number of sub-circuits
b	–	Number of parallel branches per sub-circuit
–	–	The geometry of the cooling system is based on constructional limitations

$\dot{m}_b$ – mass flow per cooling branch, [kg/s].
C_p – specific heat at constant pressure [J/kgK].
ΔT – Temperature difference between boiling temperature and current temperature of helium [–].

Normally, the helium is provided by the gravitational force from the phase separator located above the heat exchanger, helium is already near the boiling temperature and the ΔT is small.

After the helium reaches the boiling temperature the additional heat input causes helium evaporation and can be expressed by Equation (2). This equation sequentially calculates the vapour fraction change throughout the piping, each calculation node at a time.

$$\dot{Q}_n = L_{He}\dot{m}_b(x_n - x_{n-1}) \rightarrow x_n \tag{2}$$

where:
$\dot{Q}_n$ – unit heat per element [W].
L_{He} – latent heat of helium [J/kg].
x_{n-1}, x_n – inlet and outlet vapour fraction of the element, respectively [-].
$\dot{m}_b$ – mass flow per cooling branch, [kg/s].

4.4. Pressure drop

After the vapour fraction at each calculational node was calculated, it can be used for the calculation of the pressure drop of each element of the piping.

Since the homogeneous model is employed, the pressure drop was calculated based on the Darcy–Weisbach relation which is used for a single-phase flow [38]. Nevertheless, to include two-phase influence, it is necessary to include a correction factor, which is referred to as a two-phase multiplier. In this case, the two-phase multiplier was determined using a correlation corresponding to the homogeneous model [31]. The two-phase multiplier for the homogenous model is calculated using Equation (3).

$$\phi_{lo} = \left(1 + x_{n-1}\left(\frac{\rho_L}{\rho_V} - 1\right)\right)\left(1 + x_{n-1}\left(\frac{\mu_L}{\mu_V} - 1\right)\right)^{-0.25} \tag{3}$$

where:
ϕ_{lo} – two-phase multiplier [-].
ρ_L – density of saturated liquid at a given temperature [kg/m^3].
ρ_V – density of saturated vapour at a given temperature [kg/m^3].
μ_L – dynamic viscosity of saturated liquid at a given temperature [kg/m^3].
μ_V – dynamic viscosity of vapour at a given temperature [kg/m^3].

It should be highlighted that the experimental study demonstrated by B. Baudouy in [22] proves that Friedel's correlation formulated for the separate model is also accurate, which was validated against experimental results. In spite of that, Baudouy [22] recommends using the homogeneous model to calculate the two-phase multiplier because of its simplicity.

4.4.1. Serpentine model

As it was mentioned before, pressure drop inside the cryogen stream was calculated using the Darcy–Weisbach equation with the addition of the two-phase multiplier. The pressure drop for the single branch of the serpentine model was calculated using Equation (4)

$$\Delta p_{ns} = \phi_{lo}\left(\frac{l_n}{D}\lambda + \zeta\right)\left(\frac{8\dot{m}_b^{\,2}}{\pi^2 D^2 \rho_m}\right) \tag{4}$$

where:
Δp_{ns} – pressure drop in a single element of a serpentine branch [Pa].
ϕ_{lo} – two-phase multiplier [-].
D – flow channel diameter [m].
l_n – flow channel length [m].
λ – linear friction factor [-].
ζ – local losses factor [-].
ρ_m – two-phase mixture average density [kg/m^3].
g – gravitational acceleration [m/s^2].

It is worth mentioning, that the pressure drop equation for a single element of the serpentine model does not include the gravity factor which expresses the changing height along the cooling path. This is caused by the complexity of the geometrical model i.e., cooling tubes are inclined in relation to more than one geometrical plane. The gravity factor is included at a later stage of the calculations.

The outlet vapour fraction itself does not affect the working performance of the cooling loop, although it may be an indication of the correctness of the homogeneous model simplifications. T. Haruyama et al. [21] demonstrate that for inlet vapour fraction above 70 %, neither the homogeneous nor the separated model is consistent with the experimental results. It is worth noting that the vapour fraction at the outlet does not depend on the geometry of the cooling loop as shown in Equation (2).

4.4.2. Vertical model

The pressure drop calculations for a single element of the vertical model consist of Darcy- Weisbach and the gravitational components, as expressed in Equation (5). The latter is determined regarding the elementary height of the single element based on its elementary length (mesh size) and its inclination φ which is shown in Fig. 10.

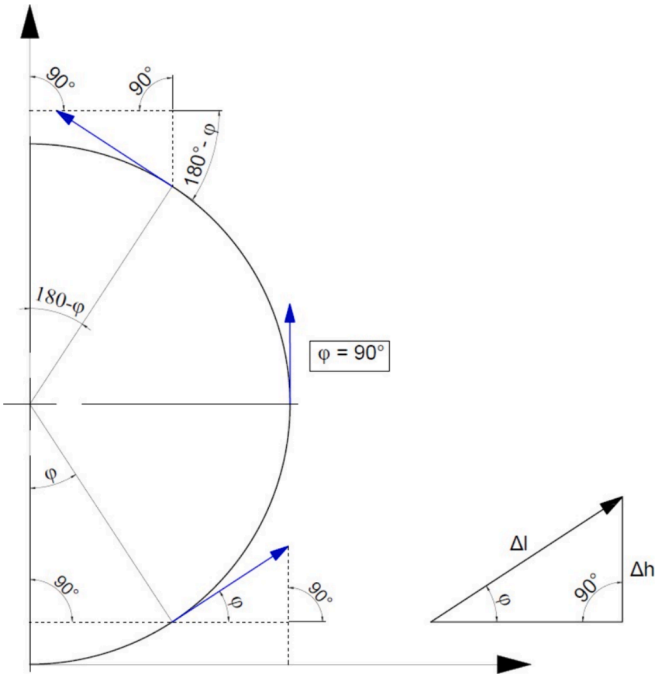

Fig. 10. Geometrical representation of the vertical cooling path.

$$\Delta p_{nv} = \phi_{lo}\left(\frac{l_n}{D}\lambda + \zeta\right)\left(\frac{8\dot{m}_b{}^2}{\pi^2 D^2 \rho_m}\right) + \rho_m g l_n \sin\varphi \quad (5)$$

where:

Δp_{nv} – pressure drop in a single element of a vertical model branch [Pa].

ϕ_{lo} – two-phase multiplier [-].

D – flow channel diameter [m].

l_n – flow channel length [m].

λ – linear friction factor [-].

ζ – local losses factor [-].

ρ_m – two-phase mixture average density [kg/m^3].

g – gravitational acceleration [m/s^2].

φ – The angle of the pipe section from the horizontal [deg].

4.5. The height of the phase separator placement

As mentioned above, the homogeneous model allows using the communicating vessel principle to determine the height of the phase separator placement. This variable is essential for the thermosiphon operation because it provides the head pressure to compensate for the pressure drop along the cooling path.

4.5.1. Serpentine model

Since the pressure change caused by the level difference of the serpentine geometry tubing was not included in the pressure drop formula for a single element – Equation (4), it needs to be included while formulating the equilibrium equation for communicating vessels. Equation (6) was implemented to determine the height of phase separator placement. It is worth noting that acceleration pressure drop is not included since its value is negligible compared to frictional and gravitational components [16,20].

$$\Delta P_{mg} + \rho_{av} g h_{mg} + \rho_2 g(h_i - h_{mg}) = \rho_L g h_i \quad (6)$$

where:

ΔP_{mg} – total flow pressure drop that results from the cumulative pressure drops across all linear elements [Pa].

ρ_{av} – average helium density across cooling loop [kg/m^3].

h_{mg} – the magnet height [m] (see Figure 4.3).

$\rho_{av} g h_{mg}$ – the gravitational pressure change within the cooling loop [Pa].

ρ_2, ρ_L – densities of the outlet mixture and the pure liquid helium, respectively [kg/m^3].

h_i – the height of phase-separator placement above the magnet floor (see Fig. 11) [m].

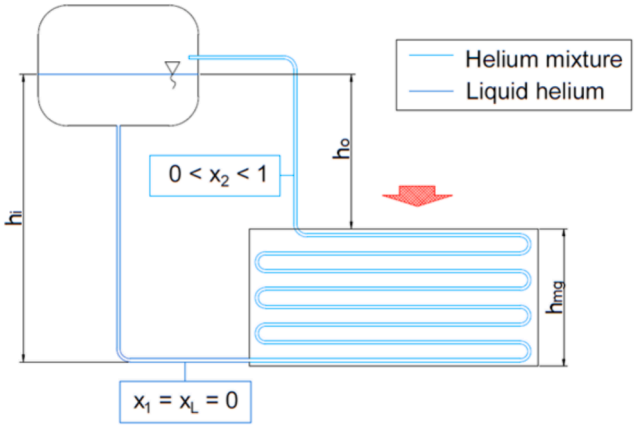

Fig. 11. The simplified scheme of the cooling circuit including geometrical relations.

4.5.2. Vertical model

Since in the vertical model, pressure drop calculation (Equation (5), the gravitational pressure change has been already included in the pressure drop formula, thus there is no need to add it to the equilibrium equation for communicating vessels [10]. The equation used to determine the phase separator height is presented below (Equation (7)). In this case, the acceleration pressure drop is also neglected. In the case of the vertical model, the gravitational component of the pressure drop is dominant, which comes from relatively short cooling pipes compared to the height of the cold mass.

$$\Delta P_{mg} + \rho_2 g(h_i - h_{mg}) = \rho_L g h_i \quad (7)$$

5. Results

5.1. Parameters for the nominal operation

The first step of the calculations using the developed software was to define the nominal operating conditions of the cooling loop and the mesh size. As the paper focuses mainly on the hydraulic effects, thermal equilibrium between helium and the inner wall of the cooling tube was assumed. This paper shows how to design the geometry of the hydraulic system to ensure a certain mass flow in the cooling loop. Therefore, the same mass flow per single cooling tube was assumed to facilitate the comparison of two heat exchangers. The heat load of the magnet is calculated based on the value of radiation heat flux of 0.2 W/m^2, i.e., the design value for the Compact Muon Solenoid [8], and the radiation surface area of the cold mass. The magnet is foreseen to be cooled using liquid helium at a slight overpressure (130 kPa). Based on this information, the input to the computational tool is formulated and presented in Table 4.

Table 5 presents the exemplary calculation results that compare the calculated pressure drop and the needed height of the phase separator placement above the magnet floor for achieving the continuous helium flow through the cooling circuit during the nominal operational condition of the magnet. The division of the cooling circuit into several subcircuits and subsequently a few parallel-connected branches significantly reduces the pressure drop within the system and thereby the height of the phase separator placement. This is expected and caused by the decrease in the frictional component of the pressure drop.

The height of the phase separator placement greatly influences the further stage of the thermosiphon-based cooling systems design. The first issue is the longer the transfer line the greater the heat load transferred to it. For a very long transfer line, due to non-zero heat loads through the thermal insulation, one cannot assume the vapour fraction at the inlet of the heat exchanger to be equal to 0. Secondly, given the geometrical constraints, for example in the underground caverns of detectors such as ATLAS and CMS [7,32], it is important to avoid the

Table 4
Input to the calculation programme.

Variable	Serpentine model	Vertical model	Unit
Operating temperature of helium	4.5	4.5	K
Operating static pressure	130	130	kPa
Vapour fraction at the inlet	0	0	–
Height of the magnet	2	2	m
Heat load for the entire cooling system	100	100	W
Number of sub-circuits	1	4	–
Number of parallel branches per sub-circuit	2	10	–
Branch internal diameter	18	18	mm
Heat load per branch	50	2.5	W
Outflow from the dewar	20	400	g/s
Mass flow in the single branch	10	10	g/s
Mesh size	0.001	0.001	m

Table 5
Calculation results for both geometrical configurations.

Variable	Serpentine model	Vertical model	Unit
Vapour fraction at the outlet	0.286	0.014	–
Pressure drop	11.3	7.5	kPa
Height of the phase separator placement	11.45	5.01	m

placement of a phase separator at an unnecessarily large height with respect to the cold mass. Therefore, it is attractive to reduce the required pressure drop through the heat exchanger and thus the height of the phase separator.

5.2. Pressure drop over the diameter of the cooling tubes and mass flow

The described engineering approach allows to design of the geometry of thermosyphon-based cooling systems to achieve a desired mass flow. Fig. 12 and Fig. 13 show the relation between pressure drop and the diameter of the cooling tubes for increasing mass flow in the thermosiphon-based cooling system respectively for the serpentine and vertical geometry models. The graphs were plotted based on the data given in Table 4.

It is noticeable that the diameter of the flow channel plays an important role in the design of any hydraulic system, i.e., the pressure drop increases with decreasing pipe diameter. The dynamics of this drop can be explained by several factors. Among others, the pressure drop is determined based on the friction factor reversely dependent on the Reynolds number which varies as a function of diameter. The bigger the flow channel, the smaller the Reynolds number which establishes the flow regime. For the laminar flow, the friction factor does not depend directly on the flow channel diameter, unlike the turbulent flow. The transition between those two regimes is represented by the inflexion points of the pressure drop curves. Another relation presented in Fig. 12 and Fig. 13 is the dependency of the pressure drop on the mass flow. For greater mass flow, the pressure drop reaches higher values. However, the bigger the diameters, the difference decreases. For the largest diameters, mass flow influence can be considered negligible. This trend can be explained by the continuity equation where once the mass flow increases, the fluid flows respectively faster which corresponds to bigger friction losses.

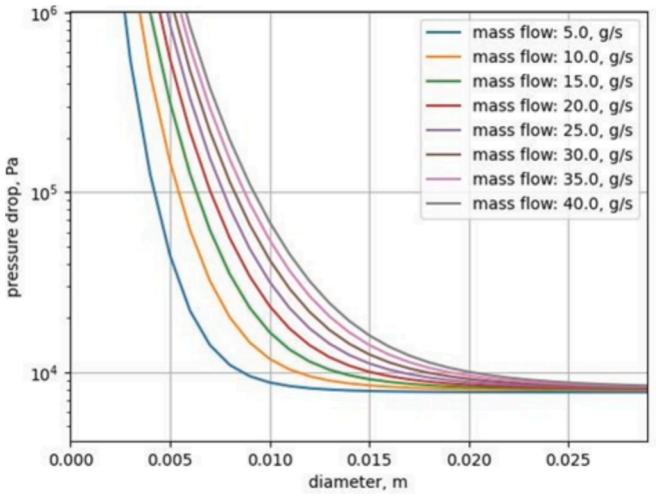

Fig. 13. Pressure drop over the diameter of cooling tubes and mass flow for the vertical model.

5.3. Height of the phase separator placement over mass flow and the diameter of the cooling tubes

The first step in the cryogenic distribution system design for the thermosiphon-based cooling loop is to optimize the height of the phase separator placement. This variable corresponds to the head pressure that needs to be provided to the system to compensate for pressure drop in the heat exchanger and create mass flow in the cooling tubes. The relation between the vertical placement of the phase separator above the magnet floor and mass flow for different pipe diameters is shown in Fig. 14 and Fig. 15. The graphs were plotted based on the data given in Table 4.

Equation (6) and Equation (7) show, that the relation between the pressure drop and the height of the phase separator is linear which introduces similar dependency trends in terms of the most relevant parameters such as mass flow and diameter of cooling tubes. This only confirms that the proper determination of the diameter of the cooling tubes is a factor of vital importance for the design process.

6. Summary

The focus of this paper is on consolidating the collected information

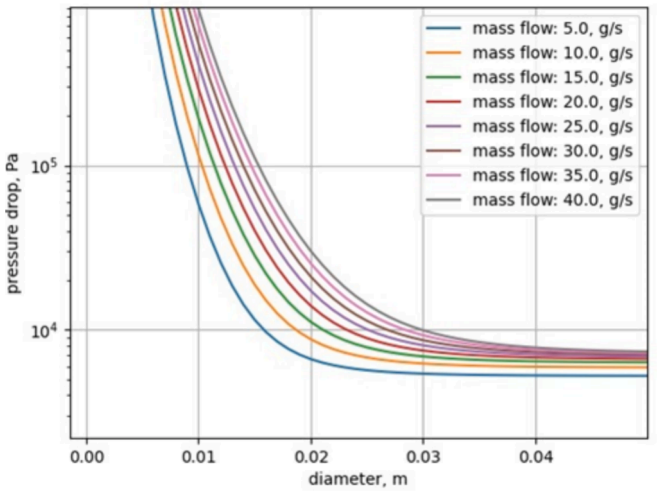

Fig. 12. Pressure drop over the diameter of cooling tubes and mass flow for the serpentine model.

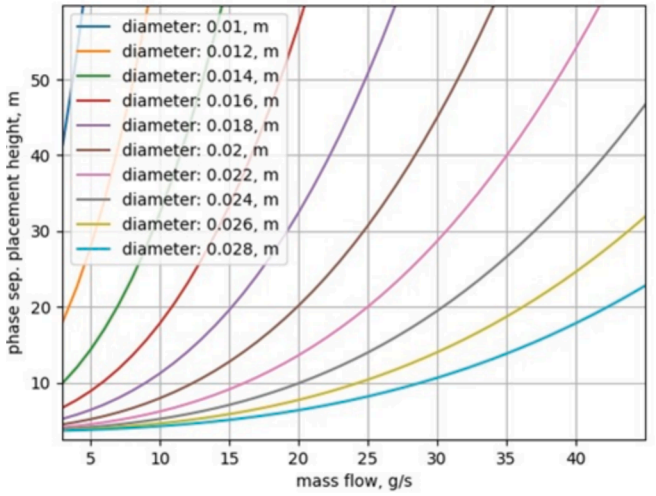

Fig. 14. The height over the mass flow and the diameter of the cooling tubes for the serpentine model.

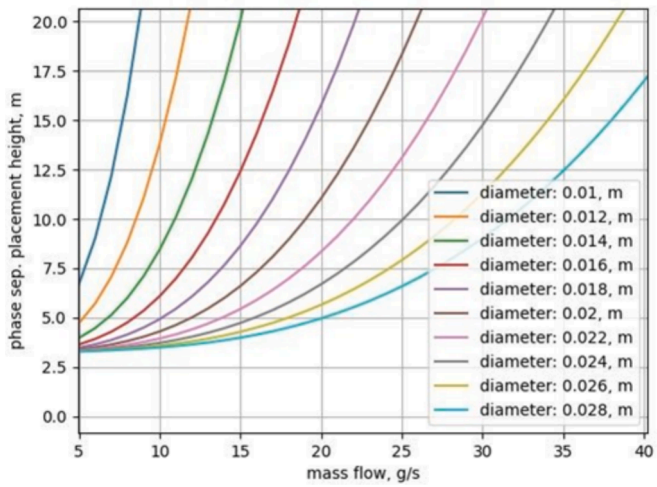

Fig. 15. The height over the mass flow and the diameter of the cooling tubes for the vertical model.

on thermosiphon-based cooling systems for LTS devices. A simplified mathematical model was formulated and subsequently used to perform hydraulic calculations on two cooling circuits of different geometries. An engineering computational tool was created and will be published as open-source software after the experimental part of the project. In this study, two spatial orientations of cooling tubes were analysed and compared: vertical and horizontal, also referred to as serpentine. A significant challenge in these calculations is determining the optimal diameters for the cryogenic tubes and establishing the minimum vertical placement of the phase separator. Both parameters influence the operation of the cooling system by affecting the pressure gradient present in individual components during system operation. This is crucial, as the differential pressure gradient within the thermosiphon tubes is the sole driving force propelling helium. When designing, it is paramount to consider both the required helium flow and the amount of heat that the cooling loop needs to collect from the solenoid.

CRediT authorship contribution statement

Weronika Głuchowska: Writing – review & editing, Writing – original draft, Visualization, Validation, Supervision, Software, Resources, Project administration, Methodology, Investigation, Funding acquisition, Formal analysis, Data curation, Conceptualization. **Tomasz Banaszkiewicz:** Writing – review & editing, Writing – original draft, Visualization, Validation, Supervision, Software, Resources, Project administration, Methodology, Investigation, Funding acquisition, Formal analysis, Data curation, Conceptualization. **Matthias Mentink:** Writing – review & editing, Validation, Supervision, Conceptualization. **Benoit Cure:** Writing – review & editing, Visualization, Validation, Supervision. **Alexey Dudarev:** Writing – review & editing, Visualization, Validation, Supervision. **Shuvay Singh:** Writing – review & editing, Validation, Supervision.

Declaration of competing interest

The authors declare that they have no known competing financial interests or personal relationships that could have appeared to influence the work reported in this paper.

Data availability

Data will be made available on request.

Acknowledgements

This work was supported by CERN EP R&D on Experimental Technologies (WP8 Detector Magnets) and by statutory funds from the Polish Ministry for Science and Higher Education.

References

[1] Wilson MN. Superconducting Magnets. New York: Oxford; 1983.
[2] Iwasa Y. SUPERCONDUCTING MAGNET TECHNOLOGY. In: Case Studies in Superconducting Magnets: Design and Operational Issues. Springer US; 2009. p. 1–24.
[3] Mulder T. Advancing ReBCO-CORC Wire and Cable-in-Conduit Conductor Technology for Superconducting Magnets. UT, graduation UT; 2018. Available from: https://doi.org/10.3990/1.9789036546164.
[4] Ekin J. Experimental Techniques for Low-Temperature Measurements: Cryostat Design, Material Properties and Superconductor Critical-Current Testing. Oxford University Press; 2006.
[5] Baze JM. Design, construction and test of the large superconducting solenoid ALEPH. IEEE Trans Magn 1988;24(2):1260–3.
[6] Lottin JC, Duthil R, Aleph, System C. Proceedings of the Twelfth International Cryogenic Engineering Conference; 1988. p. 117–121. Available from: 10.1016/B978-0-408-01259-1.50022-X.
[7] Yamamoto A. The ATLAS central solenoid. Nucl Instrum Methods Phys Res Sect Accel Spectrometers Detect Assoc Equip 2008;584(1):53–74.
[8] Dhanaraj N, Kashikhin V, Peterson T, Pronskikh V, Nicol T. Study of thermosiphon cooling scheme for the production solenoid of the Mu2e experiment at Fermilab. AIP Conference Proceedings. 2014 01;1573(1):400–406.
[9] Dhanaraj N, Tatkowski G, Huang Y, Page TM, Lamm MJ, Schmitt RL, et al. An analytical approach to designing a thermosiphon cooling system for large-scale superconducting magnets. IOP Conference Series: Materials Science and Engineering. 2015 nov;101(1):012142.
[10] Ma Y, Koveshnikov A, Lang D, Laxdal R, Muller N. Thermosiphon Cooling Loops for ARIEL Cryomodules. In: 18th International Conference on RF Superconductivity; 2018. p. 105.
[11] Rolando G, ten Kate HHJ, Dudarev A, Silva HPD, Vodopyanov A, Schmitt L. Thermal analysis of the cold mass of the 2T solenoid for the PANDA detector at FAIR. IOP Conference Series: Materials Science and Engineering. 2015 nov;101(1):012151.
[12] Choudhury A, Sahu S, Kanjilal D. Cryocooler-based helium liquefier using an active thermosiphon process. Cryogenics 2020;106:103040.
[13] Kirichek O. Operation of superconducting magnet with dilution refrigerator insert in zero boil-off regime. Cryogenics 2010;50:666–9.
[14] Wang C, Hartnett J. A vibration-free cryostat using pulse tube cryocooler. Cryogenics 2010;50:336–41.
[15] Huang HC. High magnetic field superconducting magnet with zero helium boil-off for nuclear magnetic resonance spectrometer. IEEE Trans Appl Supercond 2010;20(3):748–51.
[16] Lottin JC, Juster FP. Liquid helium thermosiphon for the 4 TESLA CMS solenoid. Adv Cryog Eng 1998;43:1505–11.
[17] La AD, Harpe. Boiling heat transfer and pressure drop of liquid helium-I under forced circulation in a helically coiled tube. Adv Cryogenic Eng 1969;14:170–177.
[18] Zust HK, Bald WB. Experimental observations of flow boiling of liquid helium I in vertical channels. Cryogenics 1981;21:90256–9.
[19] Sauvage-Boutar E. Observation of two-phase helium flows in a horizontal pipe. Adv Cryog Eng 1988;33:441–7.
[20] Huang X, Sciver SW. Pressure drop and void fraction of two-phase helium flowing in horizontal tubes. Cryogenics 1995;35:467–74.
[21] Haruyama T. Pressure drop of two-phase helium flowing in a large solenoidal magnet cooling path and a long transfer line. Cryogenics 1996;36:465–9.
[22] Baudouy B. Pressure drop in two-phase He I natural circulation loop at low vapor quality. nternational Cryogenic Engineering Conference proceedings. 2002;19:817–820.
[23] Visentin F, Baudouy B, Irfu. Helium two-phase flow in a thermosiphon open loop; 2009.
[24] Green MA. Helium cooling systems for large superconducting physics detector magnets. Cryogenics 1992;32:126–9.
[25] Lvovsky Y. Novel technologies and configurations of superconducting magnets for MRI. Supercond Sci Technol. 2013;26(093001).
[26] Desportes H. Superconducting magnet for EHS. IEEE Trans Magn 1981;17(1):718–21.
[27] Arp V. Single-Phase Helium Cooling Systems. In: Timmerhaus KD, editor. Advances in Cryogenic Engineering: A Collection of Invited Papers and Contributed Papers Presented at National Technical Meetings During. Springer US; 1970. p. 342–351.
[28] Vaghela H, Lakhera VJ, Sarkar B. Forced flow cryogenic cooling in fusion devices: a review. Heliyon 2021;7(1):6053.
[29] Beurthey S, Böhmer N, Brun P, Caldwell A, Chevalier L, Diaconu C, et al. MADMAX Status Report. 2020.
[30] ATLAS, Collaboration. ATLAS TDR-7; CERN/LHCC 97-19. 1997;2.
[31] Bertrand B, Anne B, Aurélien F. Modeling of a horizontal circulation open loop in two-phase helium. Cryogenics 2013;53:2–6.
[32] The CMS Collaboration et al. The CMS experiment at the CERN LHC. J Instrum. 2008;3(08).
[33] Filina NN, Weisend JG. I I. Cambridge University Press; 2011.

[34] Massoud M. Two-Phase Flow and Heat Transfer. In: Engineering Thermofluids: Thermodynamics, Fluid Mechanics, and Heat Transfer. Berlin, Heidelberg: Springer Berlin Heidelberg; 2005. p. 601–686.
[35] Emmanuil C, Sinaiski, Hydromechanics. John Wiley & Sons; 2011.
[36] Python Software Foundation. Python Language Reference, version 3.10. Available at http://www.pyt hon.org.
[37] Bell IH, Wronski J, Quoilin VS, Lemort. Pure and pseudo-pure fluid thermophysical property evaluation and the open-source thermophysical property library coolprop. Ind Eng Chem Res. 2014;53:2498–2508.
[38] Gupta SC. PEARSON Education; 2006.
[39] Allain H, Baudouy B, Madur A, Rasamimanana O, Reymond H, Mueller H, et al. Study and test of an active thermosiphon experimental set-up to validate super-FRS dipoles cooling system. IOP Conf Series: Mater Sci Eng 2019;502:012098.
[40] Hu R, Yuntao S, Qingxi Y, Zhaoxi C, Kaizhong D. Experimental study on a helium cryogenic closed loop two-phase thermosyphon with a long heat transport distance. Cryogenics 2023;136:103759.
[41] Mentink M, Sasaki K, Cure B, Deelen N, Dudarev A, Abe M, et al. Superconducting detector magnets for high energy physics. J Instrum 2023;18:T06013.
[42] Cao J, Zheng Z, Asim M, Hu M, Wang Q, Su Y, et al. A review on independent and integrated/coupled two-phase loop thermosyphons. Appl Energy 2020;280:115885.
[43] Long ZQ, Zhang P. Experimental investigation of the heat transfer characteristics of a helium cryogenic thermosiphon. Cryogenics 2013;57:95–103.